Studies of Electron Cloud Growth and Mitigation in Wigglers Using Retarding Field Analyzers

J.R. Calvey, M.G. Billing, J.V. Conway, G. Dugan, S. Greenwald, Y. Li, X. Liu,
J.A. Livezey, J. Makita, R.E. Meller, M.A. Palmer, S. Santos, R.M. Schwartz,
J. Sikora, C.R. Strohman, CLASSE, Cornell University, Ithaca, NY, USA
S. Calatroni, G. Rumolo, CERN, Geneva, Switzerland
K. Kanazawa, Y. Suetsugu, KEK, Ibaraki, Japan
M. Pivi, L. Wang, SLAC, Menlo Park, CA, USA
(Dated: October 31, 2012)

Over the course of the past four years, the Cornell Electron Storage Ring (CESR) has been reconfigured to serve as a test accelerator (CESRTA) for next generation machines, in particular for the ILC damping ring. A significant part of this program has been the installation of diagnostic devices to measure and quantify the electron cloud effect, a potential limiting factor in these machines. In particular, several Retarding Field Analyzers (RFAs) have been installed in CESR. These devices provide information on the local electron cloud density and energy distribution, and have been used to evaluate the efficacy of different cloud mitigation techniques. This paper will provide an overview of RFA results obtained in wigglers. Understanding these results provides a great deal of insight into the behavior of the electron cloud.

PACS numbers: 29.20.db, 52.35.Qz, 29.27.-a

I. INTRODUCTION

A summary of the CesrTA RFA program, as well as detailed description of measurements and simulations in a field free environment, can be found in [1]. A description of electron cloud studies in dipole and quadrupole fields can be found in [2]. This paper will focus on results obtained in wigglers instrumented with RFAs.

II. INSTRUMENTATION

A more detailed description of the design and construction of the superconducting wigglers and their RFAs can be found in [3]; here we present only a brief overview.

In 2008, the L0 straight section of CESR was completely reconfigured for the CesrTA program. The CLEO detector was removed, and six superconducting wigglers were installed. The wigglers are 8-pole super-ferric magnets with main period of 40 cm and trimming end poles, and were typically operated with a peak transverse field of 1.9 T, closely matching the ILC DR wiggler requirements.

Three of these wigglers were equipped with RFAs (Fig. 1). Each instrumented wiggler has three RFAs: one in the center of a wiggler pole (where the field is mostly transverse), one in between poles (where the field is mostly longitudinal), and one in an intermediate region (Fig. 2). These RFAs had to be specially designed to fit in the extremely narrow aperture of the wiggler magnet. They each have one retarding grid and twelve collectors. There are 240 small holes in the beam pipe to allow electrons to enter the RFA; these holes have a diameter of 0.75 mm (1/3 of wall thickness) to reduce the EMI into the RFA signals (Fig. 3).

Two generations of metallic meshes were used as the retarding grids. The first generation was made of photochemically etched 0.15 mm-thick stainless steel (SST) mesh, with an optical transparency of approximately 38%. To reduce the secondary emission from the grid, the SST meshes were coated with approximately 0.3 μm of gold. However, as described in section IV, these low efficiency grids lead to a significant interaction between the electron cloud and the RFA, complicating the interpretation of the measurements. Therefore the second generation grids were electroformed copper meshes, consisting of 15 μm wide and 13 μm thick copper wires with spacing 0.34 mm in both transverse directions and an optical transparency of approximately 92%. The electroformed copper meshes were also coated with gold (approximately 0.3 μm in thickness) via electroplating to reduce secondary electron emission.

The collectors consist of flexible copper-clad/Kapton circuit laid on top of the ceramic frames of the grids and precisely positioned with ceramic head-pins.

Over the course of the CesrTA program, four different RFA instrumented wigglers have been constructed, each with a different electron cloud mitigation. The fist two chambers, installed in fall 2008, were bare Cu and TiN coated Cu. In summer 2009, a chamber with triangular grooves on the bottom was constructed. Some of the electrons produced in the grooves will spiral into them as they move into the center of the chamber, resulting in an effective reduction of the primary and secondary electron yield. The grooves have 2mm depth and 20° angle.

The final cloud mitigation technique we have tested in a wiggler is a clearing electrode, which simply uses a DC electric field to pull electrons toward the chamber wall. The geometry of the clearing electrode is a thin stripline [4], which consists of an alumina ceramic layer on copper

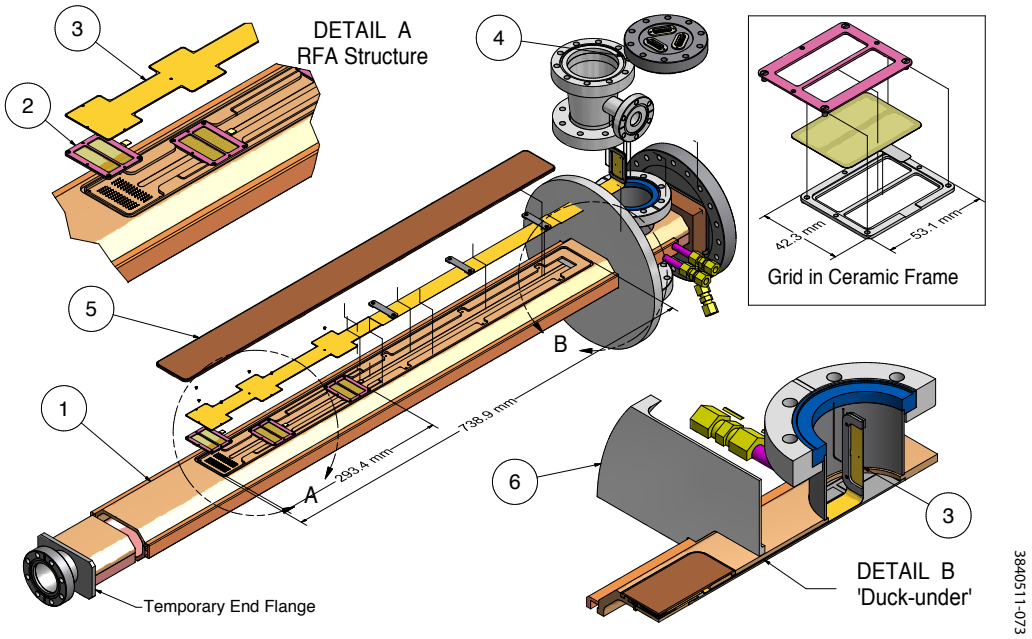

FIG. 1: Exploded View of a SCW RFA beam pipe Assembly. The key components are: (1) beam pipe top half, housing the RFAs; (2) RFA grids (see upper right inset); (3) RFA collector; (4) RFA connection port; (5) RFA vacuum cover. The 'duck-under' channel, through which the kapton flexible circuit is fed after all heavy welding is complete, is shown in detail B.

TABLE I: Locations of instrumented wiggler chambers

Dates	1W Loc	2WA Loc	2WB Loc
11/08 - 6/09	-	Cu	TiN
7/09 - 3/10	Cu	TiN	Grooves
4/10 - 12/10	Cu	TiN	Electrode
1/11 - present	Cu	Grooves+TiN	Electrode

surface (of approx. 0.2 mm in thickness) as an insulator and a thin layer of tungsten on the ceramic surface (of approx. 0.1 mm in thickness) as the electrode. These two layers were deposited via a thermal spray technique and were tightly bonded to the copper chamber. The electrode was typically operated at 400V for our measurements.

These chambers have been rotated through the three available locations in L0, to directly compare the effectiveness of each mitigation in identical photon and beam conditions. In addition, one of the wigglers was moved to a location in the 19E arc of CESR, to study the response of the RFA in a more typical photon environment. Table I gives the location of each instrumented wiggler throughout the CesrTA program. Note that in January 2011, the grooved chamber was coated with TiN, and the smooth TiN chamber was moved to 19E.

III. MEASUREMENTS

Most of the data presented here is one of two types: "voltage scans," in which the retarding voltage is varied (typically from +100 to -250V) while beam conditions are held constant, or "current scans," in which the retarding grid is set to a positive voltage (typically 50V), and data is passively collected while the beam current is increased.

Fig. 4 shows a typical voltage scan done in the center pole RFA of a Cu wiggler chamber, for a 45 bunch train of positrons at 1.25mA/bunch, 14ns spacing, and 2.1 GeV. The signal is fairly constant across all the collectors at low retarding voltage, but does become peaked at the center at high energy. There is also an anomalous spike in current at low (but nonzero) retarding voltage; this is due to a resonance between the bunch spacing and retarding voltage (see Section IV). A measurement done in the intermediate field RFA under the same beam conditions is shown in Fig. 5. It contains the spike at low retarding voltage seen in the center pole detector, and also a broader peak at higher voltage. Due to the complex 3 dimensional nature of the magnetic field at this location, this measurement is difficult to interpret.

Fig. 6 shows an example voltage scan from the grooved chamber. Because the spacing of the collectors is comparable to the distance between peaks of the grooved surface, we observe alternating dips and peaks in the collector currents.

During normal wiggler operation, no signal was ever observed in the RFAs located in the longitudinal field

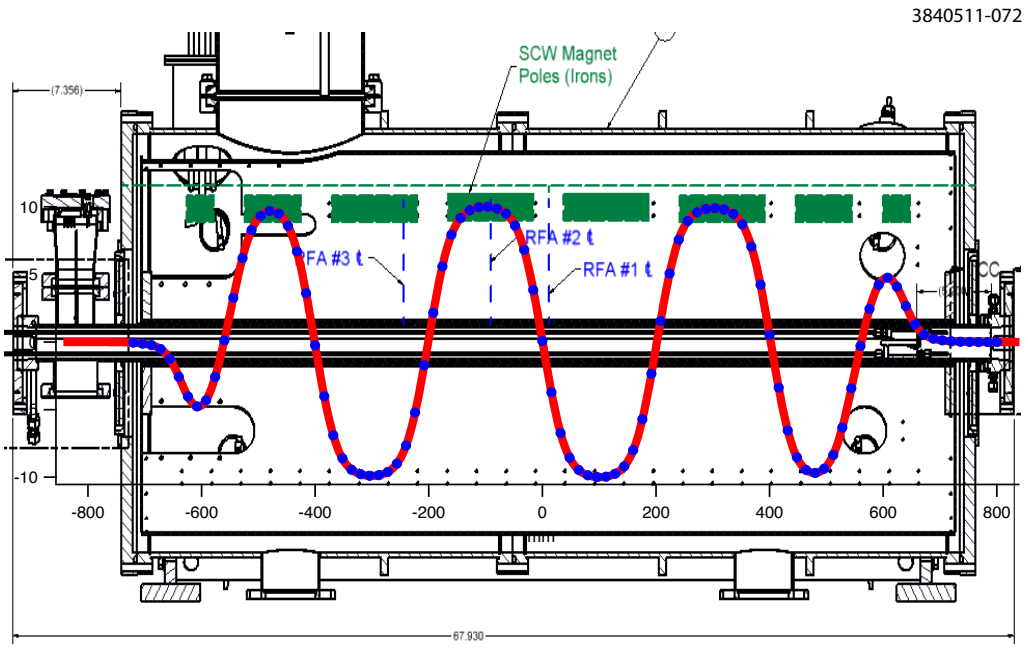

FIG. 2: Three RFAs are built into each SCW RFA beam pipe. A plot of the B-field along the wiggler (red line with blue dots) is superimposed on the drawing of the wiggler. The RFAs are located at three strategic B-field locations, as shown.

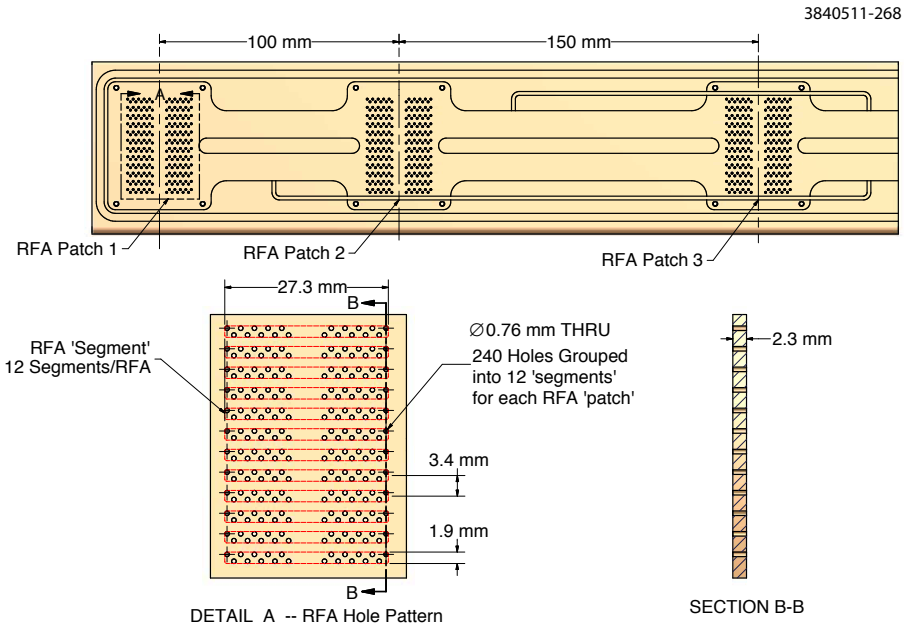

FIG. 3: Small holes are drilled through top beam pipe to allow electrons in the beam pipe drift into RFAs. There are 240 holes for each RFA, and they are grouped into 12 segments to sample transverse EC density distribution.

region. This means that no electrons in the cloud had sufficient transverse energy to cross the longitudinal field lines and reach the vacuum chamber wall. However, simulations have indicated that cloud could be trapped near the beam at these locations [5].

Signals in the intermediate field RFAs typically look similar to the center pole detectors.

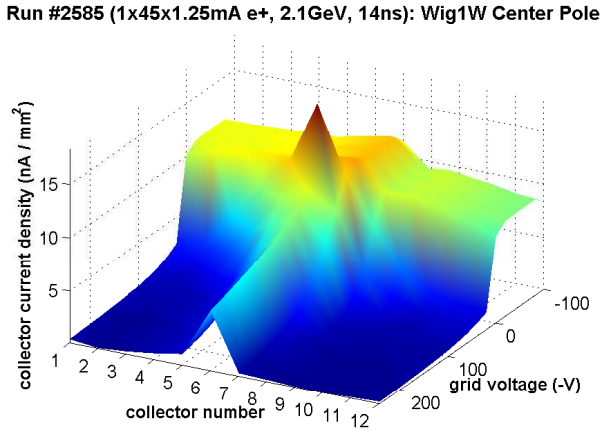

FIG. 4: Cu wiggler pole center RFA measurement: 1x45x1.25mA e+, 2.1GeV, 14ns

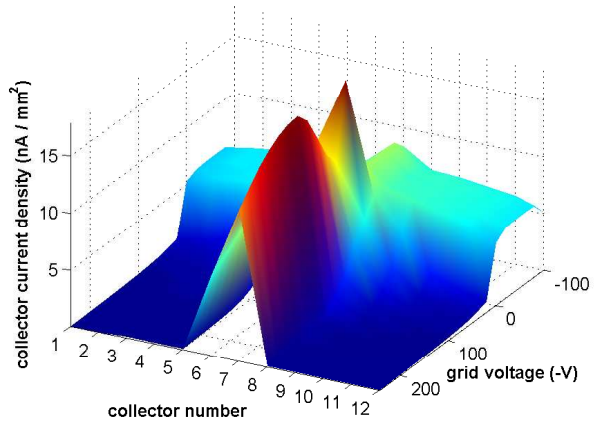

FIG. 5: Cu wiggler intermediate field RFA measurement: 1x45x1.25mA e+, 2.1GeV, 14ns

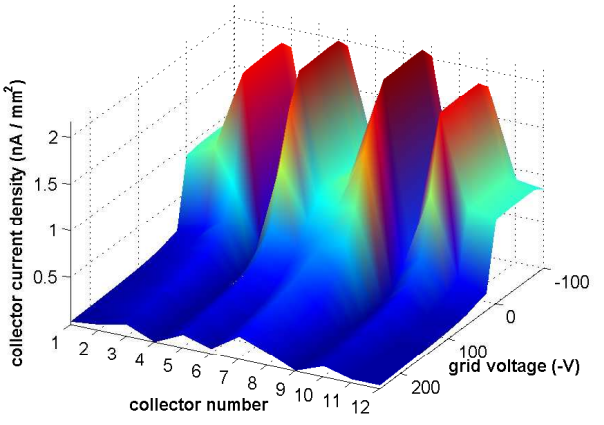

FIG. 6: Grooved wiggler pole center RFA measurement: 1x45x1.25mA e+, 2.1GeV, 14ns

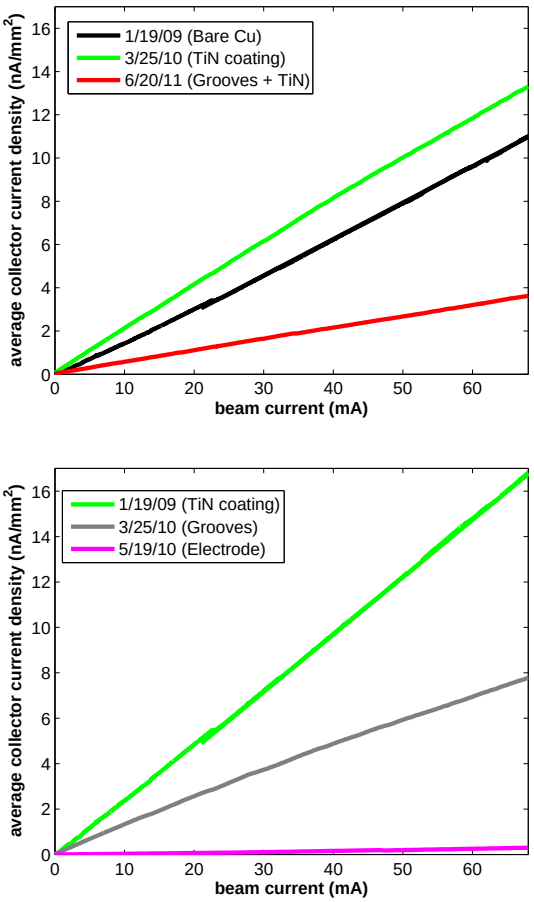

FIG. 7: Wiggler RFA mitigation comparison: 1x45 e+, 2.1GeV, 14ns. Top: 2WA location, bottom: 2WB location. The 2WB location is further downstream in the wiggler straight, and therefore has a slightly higher photon flux.

A. Mitigation Comparisons

As described above, cycling the location of the different wigglers has allowed us to compare the RFA response with different mitigation techniques at the same longitudinal position in the ring. Fig. 7 compares the average collector current (in the center pole RFA) vs beam current for different mitigation schemes, at both the 2WA and 2WB locations. These locations have slightly different photon fluxes, but as the TiN coated chamber has been installed in both, it can be used (roughly) as a reference. Note that TiN coating by itself does not appear to lead to a reduction in the wiggler RFA current relative to bare copper. Grooves do lead to an improvement, and TiN coated grooves are better still. The chamber instrumented with a clearing electrode shows the smallest signal by a wide margin, improving on TiN by approximately a factor of 50. The electrode was set to 400V for this measurement.

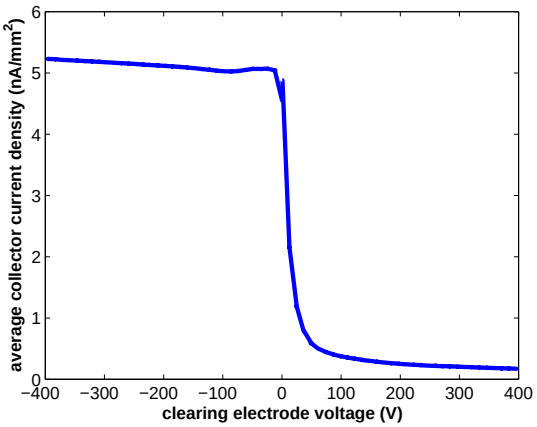

FIG. 8: Clearing electrode scan: 1x45x1mA e+, 2.1GeV, 14ns

B. Clearing Electrode Scan

Fig. 8 shows the result of varying the clearing electrode voltage on the center pole RFA. The signal is reduced by an order of magnitude with only +50V on the electrode, and continues to decrease with higher voltage. Using a negative voltage actually slightly increases the RFA signal, because the field is pushing electrons into the RFA.

C. Wiggler Ramp Studies

Very little dipole radiation is expected to reach the downstream vacuum chambers in the L0 straight, but they will be illuminated by radiation from the wigglers. Therefore, by varying the field in the wiggler magnets, we can vary the number of photons striking the wall at a given point along the straight. This will also vary the number of photoelectrons produced there, so electron cloud diagnostic devices located in L0 can provide an indirect measurement of the properties of the wiggler photons.

Fig. 9 shows the signal in three center-pole wiggler RFAs as a function of wiggler field strength. We observe a "turn on" of the signal in each detector at a specific wiggler field value. Note that the detectors that are further downstream (i.e. those with a higher s value) turn on first. This is because as the wiggler field is increased, the radiation fan becomes wider. The farther downstream a detector is, the less wide the fan must be for photons to hit at that location. This measurement can help us understand the scattering of photons in L0, since only photoelectrons produced on the top or bottom of the beam pipe can initiate the build-up of the part of the cloud detected by the RFA.

During normal operation, essentially no signal is observed in longitudinal field detectors, because there are no electrons with sufficient energy to cross the field lines. Fig. 10 shows the signal in a longitudinal field RFA (in

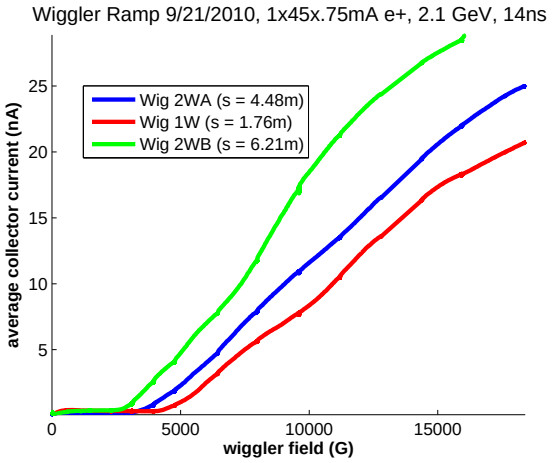

FIG. 9: Wiggler ramp measurement: 1x45x.75mA e+, 2.1GeV, 14ns

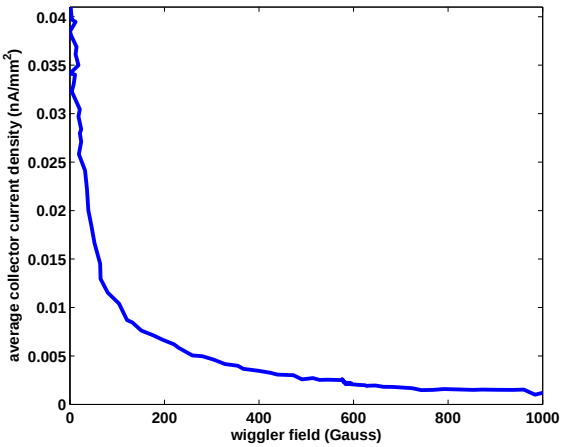

FIG. 10: Wiggler ramp measurement in longitudinal field region: 1x45x.75mA e+, 2.1GeV, 14ns

the uncoated Copper wiggler), as a function of magnetic field strength. The signal is effectively gone by 1000 Gauss, well below the 1.9T full field value.

IV. RFA MODELING

Detailed analysis of the wiggler RFA data is complicated, because of the interaction between the cloud and the RFA itself. For an example of such an interaction, see Fig. 11. It shows a voltage scan done with an RFA in the center pole of a wiggler (approximated by a 1.9 T dipole field). Here one can see a clear enhancement in the signal at low (but nonzero) retarding voltage. Since the RFA should simply be collecting all electrons with an energy more than the magnitude of the retarding voltage, the signal should be a monotonically decreasing function of the voltage. So the RFA is not behaving simply as a pas-

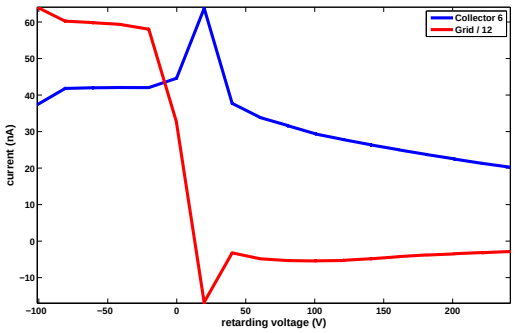

FIG. 11: Resonant enhancement in wiggler data, 45 bunches, 1.25 mA/bunch, e+, 2.1GeV. Note that there are 12 collectors, so collector 6 is one of the central ones. Also note that the grid signal is divided by 12.

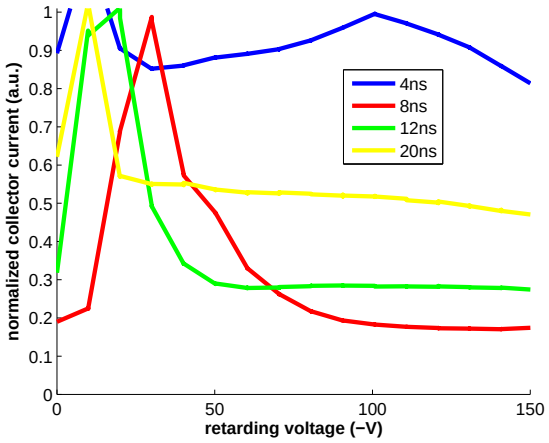

FIG. 12: Resonant spike location at different bunch spacings, 1x45x1.25 mA e+, 5GeV. Only the signal in the central collector is plotted

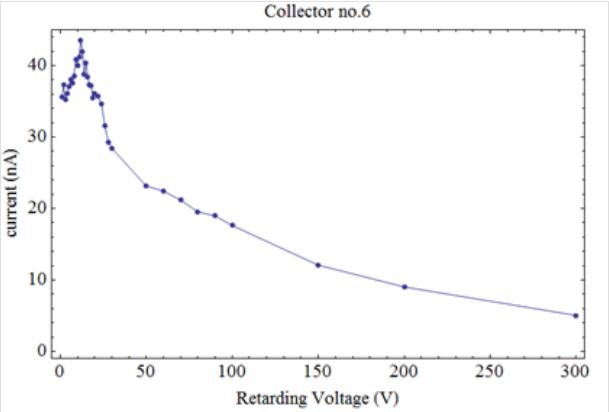

FIG. 13: POSINST simulation showing resonant enhancement, 1x45x1.2 mA e+, 2.1GeV, 14ns, central collector

sive monitor. Furthermore, the spike in collector current is accompanied by a corresponding dip in the grid current, suggesting that the grid is the source of the extra collector current.

This spurious signal comes from a resonance between the bunch spacing and retarding voltage. To understand this, consider an electron which collides with the retarding grid and generates a secondary. Because electrons are so strongly pinned to the magnetic field lines in a 1.9T field, this electron is likely to escape through the same beam pipe hole that the primary entered. In other words, the motion of the electrons is approximately one-dimensional. An electron ejected from the grid will gain energy from the retarding field before it re-enters the vacuum chamber. If it is given the right amount of energy, it will be near the center of the vacuum chamber during the next bunch passage, and get a large beam kick, putting it in a position to generate even more secondaries. The net result is a resonance condition for the retarding voltage that is inversely proportional to the square of the bunch spacing, since the shorter the bunch spacing, the more kinetic energy an electron needs to arrive at the beam in time for the next bunch passage [6]. Fig. 12 shows that this dependence is (roughly) present in the data, though the low energy spike in the 4ns data is not predicted by this model.

Motivated by these measurements, we have incorporated into POSINST a model of the RFA geared toward reproducing the geometry of the devices installed in the vacuum chambers of the CesrTA wigglers. The motion of the electrons within the RFA, including the electrostatic force from the retarding field, is tracked using a special routine. The grid is modeled realistically, and secondary electrons can be produced there, with the same secondary yield model used for normal vacuum chamber collisions. The peak secondary electron yield and peak yield energy can be specified separately for the grid.

Because the actual retarding field is included in this model, the retarding voltage must be specified in the input file, and a separate simulation must be run for each voltage desired. Fig 13 shows the result of running this simulation for a series of different retarding voltages, for one set of beam conditions. Notably, the simulation reproduces the resonant enhancement seen in the data, at approximately the same voltage (10V for 14ns spacing).

V. CONCLUSIONS

A major component of the CesrTA program has been the study of electron cloud growth and mitigation in a wiggler field environment. We have presented data from RFAs located in the center of a wiggler pole, half way between poles, and in an intermediate region. Different mitigations have been employed at the same location in CESR, and their efficacy has been directly compared. In particular, we tested a bare copper chamber, and compared it to a TiN coating, grooves, a combination of grooves and coating, and a clearing electrode. We found

the clearing electrode to be the most effective mitigation. We have also studied the response of the detectors as a function of wiggler field. Detailed analysis of the voltage scan data is complicated by a resonance between the retarding field and bunch spacing, but incorporating a complete model of the RFA into our simulation code has allowed for this effect to be modeled.

[1] J. C. et. al., Phys. Rev. ST Accel. Beams **A598**, 372 (2012).

[2] J. C. et. al., Phys. Rev. ST Accel. Beams **A598**, 372 (2012).

[3] M. Palmer, M. Billing, G. Dugan, D. Rubin, and M. Furman, Tech. Rep., LEPP, Cornell University, Ithaca, NY (2012), URL `https://wiki.lepp.cornell.edu/ilc/bin/view/Public/CesrTA/CesrTAPhaseIReport`.

[4] Y. Suetsugu, H. Fukuma, L. Wang, M. Pivi, A. Morishige, Y. Suzuki, M. Tsukamoto, and M. Tsuchiya, Nucl. Instrum. Methods Phys. Res. **A598**, 372 (2009).

[5] C. M. Celata, Phys. Rev. ST Accel. Beams **14**, 041003 (2011).

[6] J. R. Calvey, C. M. Celata, J. A. Crittenden, G. F. Dugan, S. Greenwald, Z. Leong, J. Livezey, M. A. Palmer, M. Furman, M. Venturini, et al., in *Proceedings of the 2010 International Particle Accelerator Conference, Kyoto, Japan* (2010), pp. 1970–1972, URL `http://accelconf.web.cern.ch/AccelConf/IPAC10/papers/tupd022.pdf`.